Review

Kinetic study and model of the photocatalytic degradation of rhodamine B (RhB) by a TiO₂-coated activated carbon catalyst: Effects of initial RhB content, light intensity and TiO₂ content in the catalyst

Youji Li [*], Shuguo Sun, Mingyuan Ma, Yuzhu Ouyang, Wenbin Yan

College of Chemistry and Chemical Engineering, Jishou University, Jishou 416000, Hunan, PR China

Abstract

Heterogeneous photocatalysis has proved to be a useful tool for the degradation of water pollutants over the past 30 years. Despite notable achievements in this domain, a more satisfactory and accurate kinetic model has to be developed further. In this work, to clarify the dependence of the apparent rate constant k_{app} of the first-order kinetics on the initial organic content, light intensity and TiO₂ content of TiO₂/AC (TiO₂-coated activated carbon, TA), the photocatalytic treatment of rhodamine B (RhB) as a model compound has been studied by using TA in suspension as a photocatalyst. The photocatalytic degradation kinetic characteristics were experimentally investigated under different reaction conditions (light intensity, initial organic content and TiO₂ content of TA). To account for the experimental results, a new kinetic model is proposed on the basis of intrinsic element reactions, which takes into account the effect of light intensity, reaction intermediates, and the absorption performance on h⁺ forming, organic compound combining with •OH and degradation rate, respectively. The new kinetic model fairly resembles the classic Langmuir–Hinshelwood equation from its expression. However, it does predict that both k_r^{-1} and K_S are linearly proportional to the reciprocal of the square root of the light intensity in a rather large intensity range. The model fits quite well with the experimental data and elucidates phenomena about the effects of the TiO₂ content of TA on the degradation rate.
© 2008 Elsevier B.V. All rights reserved.

Keywords: Kinetic model; Photocatalysis; TiO₂-coated activated carbon; Rhodamine B; Composite catalyst

1. Introduction

In recent years, there has been great interest in the use of advanced oxidation processes (AOPs) for the destruction of hazardous and refractory organic compounds, due to the high oxidation potential of active oxygen species such as •OH and O_2^{-}• which are generated from irradiated semiconductor catalyst particles [1–5]. As one such AOP, the photocatalytic oxidation of toxic organic compounds through the use of a TiO₂ semiconductor is an emerging technology. The use of the TiO₂ photocatalyst in environmental clean-up operations has been of great interest due to its non-toxic nature, photochemical stability and low cost, particularly when sunlight is used as the source of irradiation [6,7]. However, the shortcomings of conventional powder catalysts lie in the low efficiency in making use of light

irradiation, and the difficulty in separation after photocatalysis [8]. These disadvantages of TiO₂ result in a low efficiency of the photocatalytic activity in practical applications. To achieve rapid and efficient decomposition of organic pollutants and easy manipulation in a total photocatalytic process, it may be effective to load photocatalysts onto suitably fine adsorbents to concentrate the pollutants around the photocatalysts. Therefore, much recent work has focused on the preparation, as well as modification of TiO₂, and as such, some composites like SiO₂/TiO₂, ZrO₂/TiO₂ and TiO₂-coated polystyrene spheres were proposed [9–12]. In addition, composites such as TiO₂/carbon [13–15] have also been prepared. It has been reported that the combined roles of the activated carbon and TiO₂ show a synergistic effect on the efficient degradation of some organic compounds in the photocatalytic process [16]. Although the basic principles of photocatalysis over illuminated TiO₂ are well established, the model of a photocatalytic process can be quite a complicated matter, as it introduces light intensity to the classical aspects of the heterogeneous catalytic systems [17–20]. Therefore, several

* Corresponding author. Tel.: +86 7438563911; fax: +86 7438563911.
E-mail address: bcclyj@163.com (Y. Li).

Nomenclature

C_0	initial organic content
I	light intensity
$[I_i]$	the concentration of the various intermediate products of RhB degradation.
k_{app}	the apparent first-order rate constant
k_r	the reaction rate constant in a modified Langmuir–Hinshelwood model
k_1	reaction rate constant in the equation of TiO_2 irradiated to produce electron–hole pairs
k_2	reaction rate constant in the equation of electron–hole recombination to produce heat
k_3	reaction rate constant in the equation between hole and hydroxyl groups
k_4	reaction rate constant in the equation between hole and water molecules
k_5	reaction rate constant in the equation between free radical and organic molecules
k''	the reaction rate constant in equation of decomposition of the RhB by $^\bullet OH$
k_4'	product of k_4 and water molecule concentration
K_C	adsorption rate constants for RhB molecules
K_i	adsorption rate constants for the various intermediate products of RhB degradation
K_O	adsorption rate constants of the $^\bullet OH$ radicals
K_S	the adsorption rate constant in a modified Langmuir–Hinshelwood model
RhB	rhodamine B
TA	TiO_2-coated activated carbon
Θ_{OH}	fractional site coverage by $^\bullet OH$ radicals
Θ_r	fractional site coverage by the total organic molecules
Θ_{RhB}	fractional site coverage by RhB dyestuff

photocatalytic studies are currently focused on the usual issues of normal catalysis without light: degradation of pollutants, simple kinetics and mechanism reactions, and enhancement of the conditions of operation (catalyst immobilization and doped, optimal pH, etc.) [21–25]. There is another particular group, the main goal of which is the study of radiation phenomena: an intrinsic study of the functioning of the catalyst, radiation models, reactors designs taking into account the radiation path, etc. [26–34]. Most authors have studied both fields separately, and as such, little effort has been done to interconnect the two of them. Therefore, a new model is proposed by considering the influence of the reaction intermediates and light intensity on the degradation rate obtained from element reactions and photocatalytic kinetics, respectively.

The first-order kinetic expression has often been used due to its simplicity [35] with good agreement for a certain initial organic content in photocatalytic process.

$$r = -\frac{dC}{dt} = k_{app}C \tag{1}$$

in which k_{app} is the apparent first-order rate constant (with the same restriction of $C = C_0$ at $t = 0$, with C_0 being the initial content in the bulk solution after dark adsorption and t the reaction time). The kinetic behavior in which k_{app} of the first-order kinetics is affected by the initial organic content, could be commonly described in terms of a modified Langmuir–Hinshelwood model, which has been successfully used for heterogeneous photocatalytic degradation to determine the relationship between the apparent first-order rate constant and the initial content of the organic substrate [2,36], which is commonly expressed as Eq. (2):

$$r = -\frac{dC}{dt} = \frac{k_r K_S C}{1 + K_S C_0} = k_{app}C$$

$$\frac{1}{k_{app}} = \frac{1}{k_r K_S} + \frac{C_0}{k_r} \tag{2}$$

where C_0 is the initial organic content, k_r is the reaction rate constant and K_S is the adsorption rate constant.

Obviously, the reaction rate is dependent on the light intensity and absorption performance of the catalyst. Some researchers [37,38] reported a similar finding in which the light intensity affected both constants (k_r, K_S) in the L–H model. However, the rate constant k_r and adsorption constant K_S in the L–H model are independent of both factors. Although K_S reflects the adsorptive affinity of a substrate on the catalyst surface, it should not vary with the light intensity, so the virtual meanings of the parameters (k_r, K_S) in the L–H model have not been clarified [39,40]. Thus, a new model is related to these points, that is, containing initial organic content, light intensity and some parameters, which correlate with the absorbing performance of the TA catalyst (i.e. TiO_2 content of TA, due to both showing pertinency). In this way, if these points are included into the kinetic model, a novel kinetic constant independent from the light intensity and initial organic content, is realized. Meanwhile, the effect of the TiO_2 content in the TA catalyst on the degradation rate is explained by its kinetic parameters. We first investigated the kinetic characteristics of the photocatalytic degradation of (RhB) at different initial contents of RhB, light intensity and TA catalyst with different TiO_2 content in order to establish a kinetic model and insight into the relationship between the degradation rate and the TiO_2 content of TA and light intensity. Meanwhile, the following work aims to test a new kinetic model and elucidate from the data obtained that the TiO_2 content in the TA catalyst affected the photocatalytic process.

In summary, this work is focused on the behavior of a photocatalytic system operating with a TA suspension, establishing the kinetic model equations and using the data obtained to test them that concern the effect of initial organic content, light intensity and TiO_2 content of TA.

2. Materials and methods

2.1. Composite photocatalyst preparation

Commercially available activated carbon grains were used, which were produced by the vapor activation of coconut shell

and had the grain size of about 0.12 cm. Precursor solutions for TiO$_2$/AC, namely TA, were prepared by the following method. Tetrabutylorthotitanate (Aldrich, 99.9%, 17.02 ml) and diethanolamine (4.8 ml) were dissolved in ethanol. The solution was stirred vigorously for 2 h at 20 °C followed by the addition of a mixture of distilled water (0.9 ml) and ethanol (10 ml) on stirring. The resulted alkoxide solution was left at 20 °C to hydrolyze to a TiO$_2$ sol. Then, a desired amount of activated carbon grains used as the substrate, was added into the TiO$_2$ sol with a certain viscosity. After this, the sol is ultrasonicated to produce the corresponding gel. This TiO$_2$ gel-coated activated carbon was then heat treated at 250 °C for 2 h in air and then annealed at 500 °C for 2 h in a flow of high purity nitrogen. The amount of coated TiO$_2$ was adjusted by repeating the cycle of dipping and annealing.

2.2. Experimental system

The experimental system used in the study is shown in Fig. 1. A pyrex reactor cell of 28 cm height and effective volume of 280 ml is equipped with some faucets. A high-pressure air steel vase provides air to stir the reaction liquor to achieve symmetrical mixing between the catalyst and reactant. A high-pressure mercury ultraviolet lamp, fixed in the middle of the quartz cell, is used as a light source. To keep the temperature of the mixed liquor in the reactor constant, cooling water is recirculated to absorb the infrared radiation by pumping.

2.3. Experimental conditions analytical methods

RhB solution was added into the reactor cell, followed by dosing with a TA catalyst of 3.5 g l^{-1} and subsequent aeration mixing for about 30 min in dark condition in order to eliminate the effect of TA absorption on the photocatalytic rate. Then, the illumination was turned on to start the photocatalytic reaction. The suspension was sampled from the reactor cell using a glass syringe at timed intervals during degradation and centrifuged immediately for separation of the suspended solids. The clean transparent solution was analyzed by UV–vis spectroscopy (JASCOV-560UV–vis spectrophotometer) after filtration. The RhB content was measured from the absorbance at the wavelength of 556 nm by using a calibration curve. For kinetic

analysis proposes, each sample taken from the reactor was divided into three different vials and the final absorption was given by the arithmetic average over the three measurements. Repetition tests were made to achieve arithmetic average results of the photocatalytic degradation rate.

To probe the dependence of the kinetic characteristics of the photocatalytic degradation upon light intensity, initial organic content and absorption performance of the catalyst (i.e. different TiO$_2$ content of TA), a series of experiments were carried out at different photocatalytic conditions: the initial content of RhB was varied from 1×10^{-3} to 10×10^{-3} mol l^{-1}. The light intensity of UV lamp, applied in the work, was 10, 15, 25, 40 and 60 mW cm^{-2}, respectively. The aerating rate of air and reacting temperature were controlled at 56 ml s^{-1} and 25 °C, respectively. For each group of experiments at certain light intensity, five different RhB contents were applied.

3. Results and discussion

3.1. The characteristics of samples

The content of TiO$_2$ in the TiO$_2$-coated samples per doped cycle, the BET surface area and the total pore volume, including the original activated carbon, are summarized in Table 1, together with the doped cycle times. The surface area of the hybridization catalyst increases due to the doping of the surface of the activated carbon with nano-TiO$_2$ particles because of their high surface area, and decreases due to their blocking of the pore entrances on the surface of the activated carbon substrate. For the 1-doped cycle TA, because the former effect on the surface area is stronger than the latter effect, its surface area is more than the original activated carbon and increased. However, for the TA catalyst with 2- or 3-doped cycles, its surface area was decreased markedly and was decreased gradually with increasing doping cycles or TiO$_2$ content, so the absorbing performance (surface area) of TA is logically expressed by its TiO$_2$ content. The decrease of the surface area is reasonably supposed to be the fact that the effect of nanometer TiO$_2$ particles on enhancing surface area is fewer than that of their blocking. The total pore volume of the original activated carbon was 0.08768 cm^3 g^{-1}. The total pore volume of TA is smaller than that of the original activated carbon and decreases with increasing TiO$_2$ content, which could indicate that the TiO$_2$ particles take part in blocking the pore entrances. So this change in tendency of the surface area is the same as that of the total pore volume with increasing doping cycle times for the catalyst annealed at 500 °C, as shown in
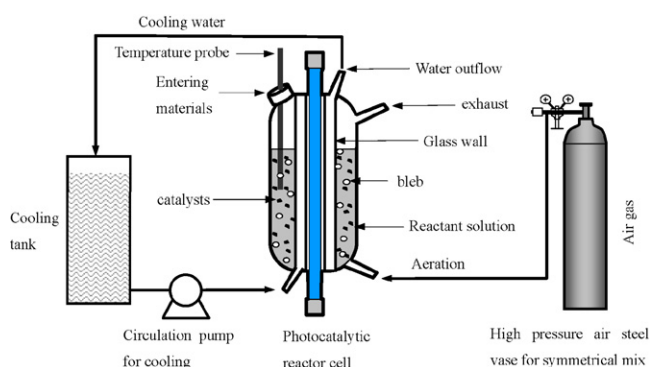

Fig. 1. Experimental system of the photocatalytic reaction.

Table 1
Characteristics of TiO$_2$-coated activated carbon (TA)

Samples	Doped cycle (times)	Content of TiO$_2$ (wt.%)	BET surface area (m^2 g^{-1})	Total pore volume (cm^3 g^{-1})
AC	–	0	435	0.08768
TA1	1	5.1	456	0.08231
TA2	2	18.3	373	0.074874
TA3	3	46.8	279	0.06458
TA4	4	62.6	271	0.05364

Table 1. Previously, the XRD patterns of TA samples, annealed at 500 °C show that the approximate ratio of the anatase to rutile phase was 2.3, and TiO_2 crystalline phase were nearly invariable with changes of TiO_2 content.

3.2. The effects of initial content of RhB, light intensity and TiO₂ content in the catalyst on photocatalytic rate

Experiments on the photocatalytic oxidation of RhB were conducted for solutions with various RhB contents: 1, 2.5, 5, 8 and 10×10^{-3} mol l^{-1}. The degradation curves of the RhB dyestuff induced by the TA photocatalyst are well fitted by a mono-exponential curve, suggesting that the degradation experiments by UV irradiation of RhB aqueous solutions containing TA follow first-order kinetics. According to Eq. (2), a plot of $\ln(C_0/C)$ versus t for all the experiments with different initial bulk concentration of RhB is shown in Fig. 2. The values of k_{app} can be obtained directly from the regression analysis of the linear curve in the plot. However, in the photocatalytic reaction system, because the reactant in solution absorbs UV light, this lowers its intensity, resulting in a decrease of the photoactivity of the hybridization catalyst. So the initial concentration of the dyestuff has a fundamental effect on the degradation rate, i.e. the kinetic rate constant decreases with increasing concentration [41]. From a practical standpoint, at the same illumination time the relative amount of RhB dyestuff decomposed is less for the much darker solutions. It is apparent from the results in Fig. 2 that the apparent rate constant decreased with increasing RhB concentration. This can be explained by the following causes: for a certain TA, the amount of active centers on the photocatalyst is finite, and the molecules of RhB are excessive in comparison with the amount of active centers on the photocatalyst thereby reducing the UV light adsorption capability of the catalyst. Thus, the photocatalytic process is influenced by the initial concentration of RhB.

Additionally, light intensity is a major factor in photocatalytic reactions, because electron–hole pairs are produced by light energy [19]. Fig. 3 shows an increase in the degradation rate constant k_{app} of RhB with increasing light intensity for a
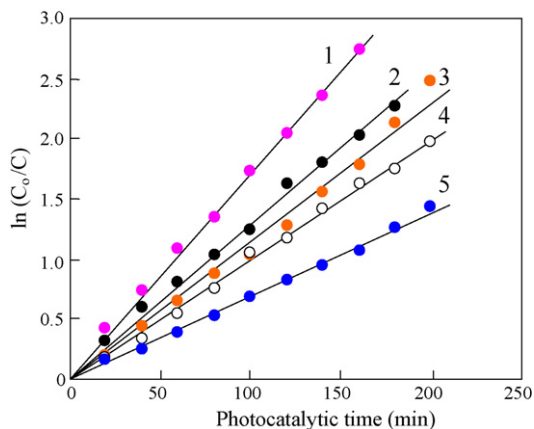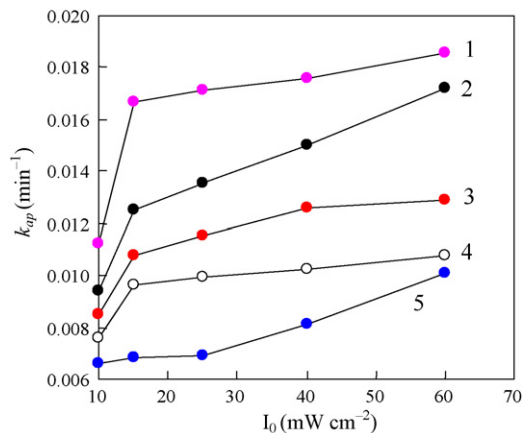

Fig. 3. The effect of light intensity on the apparent rate constant k_{app} of rhodamine B photodegradation. 1, 2, 3, 4 and 5 represent $C_0 = 1$, 2.5, 5, 8 and 10 mol l^{-1}.

certain initial organic content. For example, the decomposition rate at 60 mW cm^{-2} is faster than at 40, 25, 15 and 10 mW cm^{-2}. This is because higher light intensity provides higher energy for more TiO_2 in TA to produce electron–hole pairs. Additionally, it is evidently observed that k_{app} increases by increasing light intensity and decreasing organic content, respectively. Therefore, it is reasonably deduced that the effect of organic content on k_{app} is ascribed to the absorbing light performance of the reactant solution.

Besides the initial content of RhB solution and light intensity, the amount of TiO_2 deposited on the activated carbon support also affected the photocatalytic degradation rate of RhB. Fig. 4 shows the dependence of the apparent rate constant k_{app} determined in this way, on the TiO_2 content of TA. By comparing the dependence of k_{app} on the TiO_2 content in this figure, the apparent rate constant first increases with increasing content of TiO_2, then decreases. The relation between the RhB degradation rate and TiO_2 content follows the sequence: 46.8% > 62.6% > 18.3% > 5.1%, which means that the large quantity of photons generated by excitation of the TiO_2 species can easily contact with a sufficient amount of RhB

Fig. 2. The effect of initial concentration of rhodamine B on its photocatalytic degradation. 1, 2, 3, 4 and 5 represent $C_0 = 1$, 2.5, 5, 8 and 10 mmol l^{-1}. $I_0 = 25$ mW cm^{-1}, [TA] = 3.5 g l^{-1}, T/TA = 5.1%.
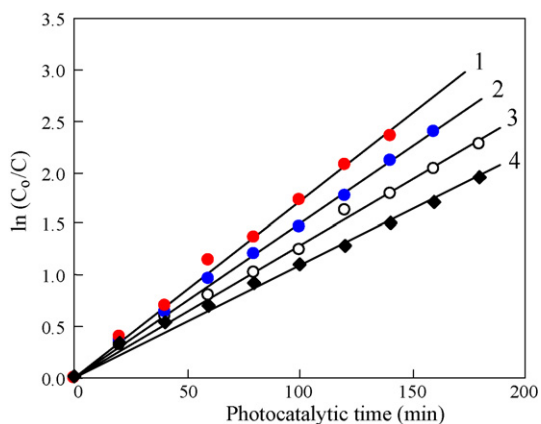

Fig. 4. The effect of TiO_2 content of TA photocatalysts on the photocatalytic degradation of rhodamine B. 1, 2, 3 and 4 represent T/TA = 46.8, 62.6, 18.3 and 5.1%, $C_0 = 2.5$ mmol l^{-1}, $I_0 = 25$ mW cm^{-1}, [TA] = 3.5 g l^{-1}.
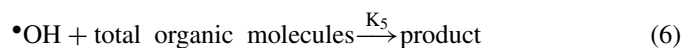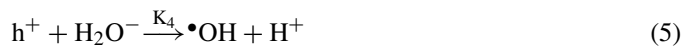
molecules, giving a high yield of photocatalyst activity. A TA catalyst showing high photoactivity should generate a sufficient amount of TiO$_2$ particles to produce photons. Meanwhile, the surface area of the activated carbon support should be sufficiently high to absorb the greatest number of RhB molecules for degradation. Because the TiO$_2$ content of TA increased with a concomitant decrease in surface area, as shown in Table 1, the TiO$_2$ content and surface area of the TA catalyst have optimum values for its high photoactivity.

3.3. Photocatalytic degradation kinetics model

Under the experimental conditions, it can be assumed that the first step in reaction is able to adsorb RhB molecules and their degradation products on the surface of TA photocatalyst, and the second step is all substrates adsorbed to be decomposed. Considering the above processes, the assumptions were followed as:

(1) Photocatalytic oxidation is mainly completed via the hydroxyl groups absorbed on the surface of the TA catalyst, which attack the organic compounds and related intermediates on the catalyst surface, which is the rate limiting step for photocatalytic degradation.
(2) The combination of H$_2$O/OH$^-$ with the photo-induced holes h$^+$ to form hydroxyl groups, and the HO$^\bullet$ radicals should be mainly formed from the adsorbed H$_2$O molecules.
(3) The combination rate of h$^+$/e$^-$ is much more than the hydroxyl forming rate of the reaction between h$^+$, H$_2$O and OH$^-$.
(4) The concentration of hydroxyl radicals is constant at a steady state (Bodenstein steady state assumption).
(5) The concentration of h$^+$ is constant at a steady state (Bodenstein steady state assumption).

Acknowledging the four reaction steps for photocatalysis, the elementary reaction equations are expressed as the following equations:

$$h\gamma \xrightarrow{K_1} h^+ + e^- \xrightarrow{K_2} \text{Heat} \tag{3}$$

$$h^+ + OH^- \xrightarrow{K_3} {}^\bullet OH \tag{4}$$

$$h^+ + H_2O \xrightarrow{K_4} {}^\bullet OH + H^+ \tag{5}$$

$${}^\bullet OH + \text{total organic molecules} \xrightarrow{K_5} \text{product} \tag{6}$$

Eq. (3) refers to the photonic activation step and depicts the recombination step, while Eqs. (4) and (5) represent the formation of the hydroxyl product, and Eq. (6) shows the transformation of the total organic molecules that contain RhB and its various intermediate degrading products to the product *P*. According to assumption 1, the photocatalytic degradation rate for the surface decomposition of RhB on TA, *r*, is represented as Eq. (7): the reaction rate

$$r = k'' \Theta_{OH} \Theta_{RhB} \tag{7}$$

where k'' is the rate constant, and Θ_{OH} and Θ_{RhB} are the fractional site coverages by $^\bullet$OH radicals and RhB dyestuff, respectively. When the light intensity and catalyst are invariable, Θ_{OH} is considered as a constant, so that Eq. (7) is a first-order kinetic model, as shown in Figs. 2 and 4. Additionally, the fractional site coverage by the RhB dyestuff is given by

$$\Theta_{RhB} = \frac{K_C C}{1 + K_C C + \sum_i K_i[I_i]} \tag{8}$$

in which K_C and K_i are the adsorption rate constants for RhB molecules and "I" refers to the various intermediate products of RhB degradation. If it is assumed that the adsorption coefficients for all organic molecules present in the reaction mixture are effectively equal, the following assumption can be made:

$$K_C C + \sum_i K_i[I_i] = K_C C_0 \tag{9}$$

$$\Theta_{RhB} = \frac{K_C C}{1 + K_C C_0} \tag{10}$$

where C_0 is the initial concentration of RhB.

On the other hand, the fractional site coverage by the $^\bullet$OH radicals is given by

$$\Theta_{OH} = \frac{K_O[^\bullet OH]}{1 + K_O[^\bullet OH]} \tag{11}$$

where K_O represents the adsorption rate constants of the $^\bullet$OH radicals.

Considering the Bodenstein steady state assumption (assumption IV) that the concentration of hydroxyl groups, [$^\bullet$OH], is constant, then

$$\frac{d[^\bullet OH]}{dt} = k_3[h^+][OH^-] + k_4[h^+][H_2O] - k_5[^\bullet OH]\Theta_T$$
$$= [h^+](k_3[OH^-] + k_4[H_2O]) - k_5\Theta_T[^\bullet OH] \approx 0 \tag{12}$$

According to assumption 2, $k_4[H_2O][h^+] \gg k_3[OH^-][h^+]$. Owing to the fact that water is the solvent (i.e. H$_2$O is in large excess) and [H$_2$O] is also constant. Consequently, [$^\bullet$OH] can be obtained as the following equation:

$$[^\bullet OH] = \frac{k_4'[h^+]}{k_5\Theta_T} \tag{13}$$

where $k_4' = k_4[H_2O]$. According to the Θ_{RhB} assumption, the fractional site coverage by the total organic molecules is given by

$$\Theta_T = \frac{K_C C + \sum_i K_i[I_i]}{1 + K_C C + \sum_i K_i[I_i]} = \frac{K_C C_0}{1 + K_C C_0}$$

The concentration of photo-induced holes, [h$^+$], can be obtained by applying assumption 5 to the following equation:

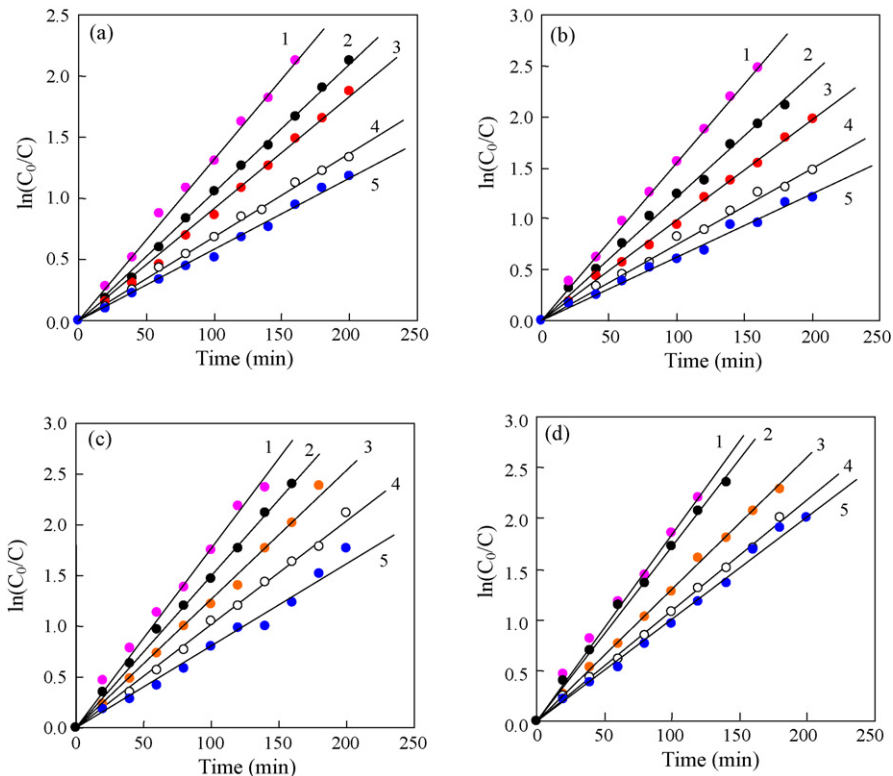$$\frac{d[h^+]}{dt} = k_1 I - k_2[h^+]^2 - k_3[h^+][OH^-] - k_4[h^+][H_2O] \approx 0 \tag{14}$$

Fig. 5. Kinetics of rhodamine B photodegradation (linear transform $\ln(C_0/C)$ vs. t) in photocatalytic experiments using TA for different concentrations of rhodamine B (1: $C_0 = 1\,\mathrm{mmol\,l^{-1}}$; 2: $C_0 = 2.5\,\mathrm{mmol\,l^{-1}}$; 3: $C_0 = 5\,\mathrm{mmol\,l^{-1}}$; 3: $C_0 = 8\,\mathrm{mmol\,l^{-1}}$; 4: $C_0 = 10\,\mathrm{mmol\,l^{-1}}$). (a): $10\,\mathrm{mW\,cm^{-1}}$, (b): $15\,\mathrm{mW\,cm^{-1}}$, (c): $40\,\mathrm{mW\,cm^{-1}}$, (d): $60\,\mathrm{mW\,cm^{-1}}$, [TA] = $3.5\,\mathrm{g\,l^{-1}}$, T/TA = 5.1%.

Rothenberger has applied laser pulse photolysis to determine the recombination rate coefficient of the separated e^- and h^+, in which k_2 is much higher than k_3 [42]. According to assumption 3, $k_2\,[h^+]^2 \gg k_3[h^+][OH^-] + k_4[H_2O][h^+]$. Consequently, $[h^+]$ has the form

$$[h^+] = \left(\frac{k_1 I}{k_2}\right)^{1/2} \tag{15}$$

Now, substitution of Eqs. (15) and (13) into Eq. (11) results in the expression in the following equation:

$$
\begin{aligned}
\Theta_{OH} &= \frac{K_O(k_4'/k_5\Theta_T)[h^+]}{1 + K_O(k_4'/k_5\Theta_T)[h^+]} \\
&= \frac{K_O(k_4'/k_5\Theta_T)(k_1/k_2)^{1/2}I^{1/2}}{1 + K_O(k_4'/k_5\Theta_T)(k_1/k_2)^{1/2}I^{1/2}}
\end{aligned}
\tag{16}
$$

By substituting Eqs. (16) and (10) into Eq. (7), the reaction rate, r, can be ultimately presented as shown in the following equation:

$$
\begin{aligned}
r &= k'' \frac{K_O(k_4'/k_5\Theta_T)(k_1/k_2)^{1/2}I^{1/2}}{1 + K_O(k_4'/k_5\Theta_T)(k_1/k_2)^{1/2}I^{1/2}} \frac{K_C C}{1 + K_C C_0} \\
&= \frac{k''(K_Ok_4'/k_5)(k_1/k_2)^{1/2}I^{1/2}((1 + K_C C_0)/K_C C_0)}{1 + (K_Ok_4'/k_5)(k_1/k_2)^{1/2}I^{1/2}((1 + K_C C_0)/K_C C_0)} \frac{K_C C}{1 + K_C C_0} \\
&= \frac{k''(K_Ok_4'/k_5)(k_1/k_2)^{1/2}I^{1/2}K_C C}{(K_Ok_4'/k_5)(k_1/k_2)^{1/2}I^{1/2} + (1 + (K_Ok_4'/k_5)(k_1/k_2)^{1/2}I^{1/2})K_C C_0} \\
&= \frac{k_r K_S C}{1 + K_S C_0}
\end{aligned}
\tag{17}
$$

where

$$k_r = \frac{k''(K_Ok_4'/k_5)(k_1/k_2)^{1/2}I^{1/2}}{1 + (K_Ok_4'/k_5)(k_1/k_2)^{1/2}I^{1/2}}$$

The reciprocal of Eq. (17) will lead to the expected relation

$$\frac{1}{k_r} = \frac{1}{k''(K_Ok_4'/k_5)(k_1/k_2)^{1/2}} \frac{1}{I^{1/2}} + \frac{1}{k''} = \frac{\alpha}{I^{1/2}} + \beta \tag{18}$$

where

$$\alpha = \frac{1}{k''(K_Ok_4'/k_5)(k_1/k_2)^{1/2}}, \qquad \beta = \frac{1}{k''}$$

$$
\begin{aligned}
K_S &= \frac{(1 + (K_Ok_4'/k_5)(k_1/k_2)^{1/2}I^{1/2})K_C}{(K_Ok_4'/k_5)(k_1/k_2)^{1/2}I^{1/2}} \\
&= \frac{K_C}{(K_Ok_4'/k_5)(k_1/k_2)^{1/2}} \frac{1}{I^{1/2}} + K_C = \frac{\eta}{I^{1/2}} + \omega
\end{aligned}
\tag{19}
$$

where

$$\eta = \frac{K_C}{(K_Ok_4'/k_5)(k_1/k_2)^{1/2}}, \qquad \omega = K_C$$

The new kinetics model above fairly resembles the classic Langmuir–Hinshelwood equation from its expression; however, k_r and K_S appear to be dependent on light intensity and reflect the adsorbing performance of TA due to certain absorbing parameters such as K_O and K_C in the model. Therefore, this kinetic model could explain the experimental phenomena of k_r and K_S
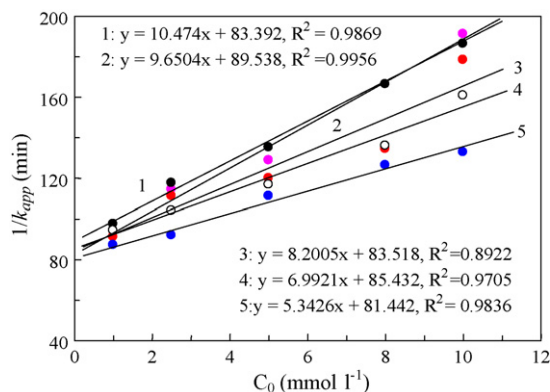
Fig. 6. Relation between $1/k_{app}$ and C_0 with different light intensity (1: $10\,mW\,cm^{-1}$, 2: $15\,mW\,cm^{-1}$, 3: $25\,mW\,cm^{-1}$, 4: $40\,mW\,cm^{-1}$, 5: $60\,mW\,cm^{-1}$).

varying with light intensity and elucidate the observed experimental results in which the initial content of RhB and TiO_2 content of TA affected the photocatalytic process.

3.4. Model fitting to the experimental data

A plot of $\ln(C_0/C)$ versus t for all the experiments with different light intensity is shown in Fig. 5. The values of k_{app} can be obtained directly from the regression analysis of the linear curve in the plot. Fig. 6 shows a plot of $1/k_{app}$ versus C_0 for different light intensity. The values of the adsorption constant, K_S, and the rate constant, k_r, are obtained by linear regression of the points calculated by Eq. (17). Granted, in Eqs. (18) and (19), the model parameters k_r and K_S both show a dependence on the square root of light intensity I. That is, $1/k_r = \alpha/I^{1/2} + \beta$, $K_S = \eta/I^{1/2} + \omega$, where α, β, η and ω are all equation coefficients determined by elementary reactions rather than light intensity, while the additional α, η and ω parameters are related to the adsorbing properties of the catalyst. Based on the assumption that the kinetic model is valid, $1/k_r$ and K_S are plotted versus $I^{-1/2}$ based on the experimental data, as shown in Figs. 7 and 8. Both $1/k_r$ and K_S are almost well correlated to $I^{-1/2}$, which supports the validity of Eq. (17). Consequently, the parameters, k_r
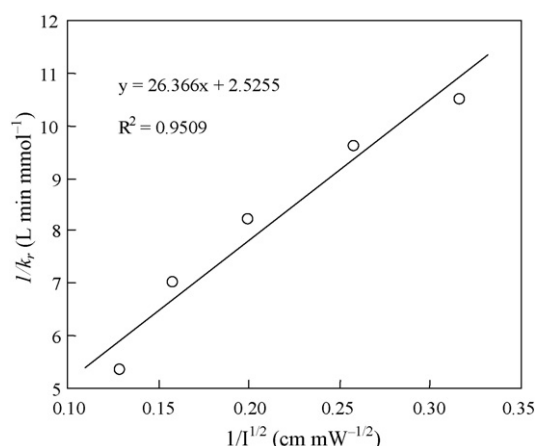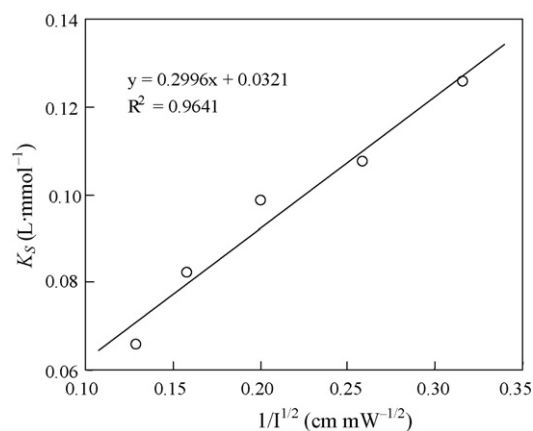

Fig. 8. Dependence of K_S on the reciprocal of the square root of light intensity.

and K_S in the present study are regressed as follows:

$$\frac{1}{k_r} = \frac{26.366}{I^{1/2}} + 2.5255 \tag{20}$$

$$K_S = \frac{0.2996}{I^{1/2}} + 0.0965 \tag{21}$$

Based on the model, $1/k_r$ and K_S are made up of two parts, one constant and the other intensity-dependent. Meanwhile, both $1/k_r$ and K_S increase with increasing $1/I^{1/2}$. Chiefly, compared to the classic L–H mode, our kinetic model shows that k_r and K_S are dependent on light intensity. This new kinetic model suggests that the dependence of, not only the reciprocal of the rate constant, $1/k_r$, but also the apparent adsorption constant K_S, on the reciprocal of the intensity results in a square root curve over a wider intensity range. Since the correlation coefficients for Eqs. (18) and (19) are high and reach 0.9509 and 0.9641, respectively, these equations for the results in Figs. 7 and 8 fit quite well with the experimental data. Furthermore, we show that some predictions coincide well with the experimental results and indicate the effects of light intensity on the rate constant and adsorbing constant by using both equations for the present investigation.

3.5. The relationship between TiO_2 content, adsorbing property of photocatalyst and its photoactivity

Under the same experimental conditions, Eqs. (20) and (21) with different constants were obtained for the TA catalyst with different TiO_2 contents, as shown in Table 2. The dependence of the rate constant k_r and adsorption constant K_S of TA was determined based on the TiO_2 content of TA when the light intensity was invariable. By comparison, at the same light intensity in this table, it is obvious that the rate constant k_r first increases with increasing TiO_2 content, but then decreases, and the relation between the rate constant k_r and the catalyst follows the sequence: TA3 > TA4 > TA2 > TA1, while the adsorption constant K_S decreases with increasing TiO_2 content with respect to the following sequence: TA1 > TA2 > TA3 > TA4. It can be assumed that the RhB decomposition rate for the TA catalyst is mostly determined by the TiO_2 particles. This may be caused by

Fig. 7. Dependence of $1/k_r$ on the reciprocal of the square root of light intensity.

Table 2
The rate constant k_r equation and the adsorption constant K_S equation of rhodamine B photodegradation with different TA catalysts, and corresponding parameter values and correlation coefficient (R^2) in both equations

Samples	k_r equation	k''	$\frac{K_O k_4'}{k_5}\left(\frac{k_1}{k_2}\right)^{1/2}$	$R^2(k_r)$	K_S equation	K_C	$\frac{K_O k_4'}{k_5}\left(\frac{k_1}{k_2}\right)^{1/2}$	$R^2(K_S)$
TA1	$\frac{1}{k_r} = \frac{26.366}{I^{1/2}} + 2.5255$	0.396	0.10	0.9509	$K_S = \frac{0.2996}{I^{1/2}} + 0.0321$	0.032	0.11	0.9641
TA2	$\frac{1}{k_r} = \frac{24.813}{I^{1/2}} + 2.1074$	0.475	0.08	0.9486	$K_S = \frac{0.2462}{I^{1/2}} + 0.0185$	0.019	0.07	0.9731
TA3	$\frac{1}{k_r} = \frac{19.427}{I^{1/2}} + 1.3856$	0.722	0.07	0.9838	$K_S = \frac{0.1959}{I^{1/2}} + 0.0126$	0.013	0.06	0.9914
TA4	$\frac{1}{k_r} = \frac{22.185}{I^{1/2}} + 1.7389$	0.695	0.06	0.9673	$K_S = \frac{0.1627}{I^{1/2}} + 0.0087$	0.009	0.05	0.9753

the fact that the RhB molecules have to be first adsorbed into the activated carbon layer and then allowed to migrate to the surface of the TiO$_2$ particles. For the TA catalyst, the degradation rate mainly depends on the TiO$_2$ content, but the surface area of the catalyst is also an important factor affecting the photoactivity of the catalyst. For the TA1 catalyst with 5.1% TiO$_2$ content, the exceptionally high adsorption constant showed a lowered degradation rate presumably due to the low TiO$_2$ content. The highest rate constant was observed for the sample TA3, which contained 46.8% TiO$_2$. The rate constant was found to increase gradually for catalysts with a TiO$_2$ content below 46.8%, which is reasonably supposed to be due to the increased amount of TiO$_2$ particles. After passing a maximum, the rate constant decreased with increasing TiO$_2$ content, which may be due to the decreasing amount of adsorbed RhB, which drastically decreased as a result of the reduced surface area.

According to Eq. (18), k'' and $(K_O k_4'/k_5)(k_1/k_2)^{1/2}$ equate to $1/\beta$ and β/α, respectively. Meanwhile, K_C and $(K_O k_4'/k_5)(k_1/k_2)^{1/2}$ equate to ω and ω/η from Eq. (19), respectively. The coefficient values are listed in Table 2 for different TA catalysts. The rate constant k'' first increases with increasing TiO$_2$ content in TA, but then decreases, which is consistent with the relation between k_r and the TiO$_2$ content of TA. Meanwhile, both K_C and K_S showed the same changing trends with increasing TiO$_2$ content in TA. Furthermore, the $(K_O k_4'/k_5)(k_1/k_2)^{1/2}$ values respectively calculated using Eqs. (18) and (19), are nearly equal and decrease with increasing TiO$_2$ content in TA. These prove that the models fit quite well with the experimental data and it is fairly rational for the above assumptions.

4. Conclusions

The kinetic characteristics of the photocatalytic degradation of rhodamine B (RhB) by a TiO$_2$-coated activated carbon (TA) catalyst were experimentally investigated with respect to the initial RhB content, different light intensities, and different TiO$_2$ contents in the TA catalyst. The kinetic characteristics were ascertained to follow a first-order model, however, the dependence of the apparent rate constant k_{app} on the light intensity, initial content of RhB and the TiO$_2$ content in the TA catalyst was observed. To account for the experimental findings, a new kinetic model, which fairly resembles the classic Langmuir–Hinshelwood equation from its expression, was proposed on the basis of intrinsic element reactions. This correlates the light intensity as a function of the parameters in the new model and further predicts that both $1/k_r$ and K_A are linear with respect to the reciprocal of the square root of the intensity over a wide intensity range. The validity of the model was partly proved by fitting it to experimental data obtained under various incident light intensities, initial organic contents, and TA catalysts with different TiO$_2$ content. This indicates that the kinetic model is rationally deduced on the basis of some valid assumptions.

References

[1] C.P. Huang, C. Dong, Z. Tang, Advanced chemical oxidation: its present role and potential future in hazardous waste treatment, Waste Manage. 13 (1993) 361–377.

[2] K. Tennakone, C.T.K. Tilakaratne, I.R.M. Kottegoda, Photomineralization of carbofuran by TiO$_2$-supported catalyst, Water Res. 31 (1997) 1909–1912.

[3] W. Choi, A. Termin, M.R. Hoffmann, The role of metal ion dopants in quantum-sized TiO$_2$: correlation between photoreactivity and charge carrier recombination dynamics, J. Phys. Chem. 98 (1994) 13669–13679.

[4] D.F. Ollis, E. Pelizzetti, N. Serpone, Photocatalyzed destruction of water contaminants, Environ. Sci. Technol. 25 (1991) 1522–1529.

[5] G. Mills, M.R. Hoffmann, Photocatalytic degradation of pentachlorophenol on titanium dioxide particles: identification of intermediates and mechanism of reaction, Environ. Sci. Technol. 27 (1993) 1681–1689.

[6] A.A. Khodja, T. Sehili, J.F. Pilichowski, P. Boule, Photocatalytic degradation of 2-phenylphenol on TiO$_2$ and ZnO in aqueous suspensions, J. Photochem. Photobiol. A: Chem. 141 (2001) 231–239.

[7] D. Chen, A.K. Ray, Photodegradation kinetics of 4-nitrophenol in TiO$_2$ suspensions, Water Res. 32 (1998) 3223–3234.

[8] M. Holgado, A. Cintas, M. Ibisate, C.J. Serna, C. Lopez, F. Meseguer, Three-dimensional arrays formed by monodisperse TiO$_2$ coated on SiO$_2$ spheres, J. Colloid Interface Sci. 229 (2000) 6–11.

[9] Y. Xu, W. Zheng, W. Liu, Enhanced photo catalytic activity of supported TiO$_2$: dispersing effect of SiO$_2$, J. Photochem. Photobiol. A: Chem. 122 (1999) 57–60.

[10] S. Fukahori, H. Ichiura, T. Kitaoka, H. Tanaka, Removal of indoor po11utants under UV irradiation by a composite TiO$_2$-zeolite sheet, Appl. Catal. B: Environ. 46 (2003) 453–462.

[11] H. Tada, A. Hattori, Y. Tokihisa, A patterned-TiO$_2$/SnO$_2$ bilayer type photocatalyst, J. Phys. Chem. 104 (2000) 4587–4592.

[12] Y. Liu, A. Wang, R. Claus, Layer-by-layer electrostatic self-assembly of nanoscale Fe3O4 particles and polyimide precursor on silicon and silica surfaces, J. Phys. Chem. 101 (1997) 1385–1997.

[13] B. Tryba, A.W. Morawaki, M. Inagaki, A new route for preparation of TiO$_2$-mounted activated carbon, Appl. Catal. B: Environ. 46 (2003) 453–462.

[14] H. Uchida, S. Itoh, H. Yoneyama, Photocatalytic decomposition of propyzamide using TiO$_2$ supported on activated carbon, Chem. Lett. 22 (1993) 1995–1998.

[15] D.K. Lee, S.C. Kim, I.C. Cho, S.J. Kim, S.W. Kim, Photocatalytic oxidation of microcystin-LR in a fluidized bed reactor having TiO$_2$-coated activated carbon, Purif. Technol. 34 (2004) 59–66.

[16] D.K. Lee, S.C. Kim, S.J. Kim, I.S. Chung, S.W. Kim, Photocatalytic oxidation of microcystin-LR with TiO$_2$-coated activated carbon, Chem. Eng. J. 102 (2004) 93–98.

[17] M.A. Fox, M.T. Dulay, Heterogeneous photocatalysis, Chem. Rev. 93 (1993) 341–357.

[18] C. Galindo, P. Jacques, A. Kalt, Photochemical and photocatalytic degradation of an indigoid dye: a case study of Acid Blue 74 (AB74), J. Photochem. Photobiol. A: Chem. 141 (2001) 47–56.

[19] C.S. Turchi, D.F. Ollis, Photocatalytic degradation of organic water contaminants: mechanisms involving hydroxyl radical attack, J. Catal. 122 (1990) 178–192.

[20] S. Irmak, E. Kusvuran, O. Erbatur, Degradation of 4-chloro-2-methylphenol in aqueous solution by UV irradiation in the presence of titanium dioxide, Appl. Catal. B: Environ. 54 (2004) 85–91.

[21] M. Sturini, E. Fasani, C. Prandi, A. Albini, Titanium dioxide-photocatalysed degradation of some anilides, Chemosphere 35 (1997) 931–937.

[22] H.D. Burrows, M.L. Canle, J.A. Santaballa, S. Steenken, Reaction pathways and mechanisms of photodegradation of pesticides, J. Photochem. Photobiol. B: Biol. 67 (2002) 71–108.

[23] M. Adachi, Y. Murata, M. Harada, S. Yoshikawa, Formation of titania nanotubes with high photo-catalytic activity, Chem. Lett. 29 (2000) 924–943.

[24] N.I. Al-Salim, S.A. Bagshaw, A. Bittar, T. Kemmitt, A.J. McQuillan, A.M. Mills, M.J. Ryan, Characterization and activity of sol–gel-prepared TiO$_2$ photocatalysts modified with Ca, Sr or Ba ion additives, J. Mater. Chem. 10 (2000) 2358–2363.

[25] M.C. Lu, G.D. Roam, J.N. Chen, C.P. Huang, Adsorption characteristics of dichlorvos onto hydrous titanium dioxide surface, Water Res. 30 (1996) 1670–1676.

[26] S. Malato, J. Blanco, A. Vidal, C. Richter, Photocatalysis with solar at a pilot-plant scale: an overview, Appl. Catal. B: Environ. 37 (2002) 1–15.

[27] Y. Ku, I.L. Jung, Decomposition of monocrotophos in aqueous solution by UV irradiation in the presence of titanium dioxide, Chemosphere 37 (1998) 2589–2597.

[28] O.M. Alfano, D. Bahnemann, A.E. Cassano, R. Dillert, R. Goslich, Photocatalysis in water environments using artificial and solar light, Catal. Today 58 (2000) 199–230.

[29] O.M. Alfano, M.I. Cabrera, A.E. Cassano, Photocatalytic reactions involving hydroxyl radical attack, J. Catal. 172 (1997) 370–379.

[30] R.J. Brandi, O.M. Alfano, A.E. Cassano, UV radiation distribution in a flat-plate photocatalytic reactor with suspended particles of titanium dioxide. Mathematical model and experimental verification, J. Adv. Oxid. Technol. 3 (1998) 213–219.

[31] R.J. Brandi, O.M. Alfano, A.E. Cassano, Rigorous model and experimental verification of the radiation field in a flat-plate solar collector simulator employed for photocatalytic reactions, Chem. Eng. Sci. 54 (1999) 2817–2827.

[32] M.I. Cabrera, O.M. Alfano, A.E. Cassano, Absorption and scattering coefficients of titanium dioxide particulate suspensions in water, J. Phys. Chem. 100 (1996) 20043–20050.

[33] M.I. Cabrera, O.M. Alfano, A.E. Cassano, Quantum efficiencies of the photocatalytic decomposition of trichloroethylene in water. A comparative study for different varieties of titanium dioxide catalysts, J. Adv. Oxid. Technol. 3 (1998) 210–218.

[34] D. Curco', S. Malato, J. Blanco, J. Gime'nez, P. Marco, Photocatalytic degradation of phenol: comparison between pilot-plant-scale and laboratory results, Solar Energy 56 (1996) 387–400.

[35] N.N. Rao, A.K. Dubey, S. Mohanty, P. Khare, R. Jain, S.N. Kaul, Photocatalytic degradation of 2-chlorophenol: a study of kinetics, intermediates and biodegradability, J. Hazard. Mater. B101 (2003) 301–314.

[36] J.B. Heredia, J. Torregrosa, J.R. Dominguez, J.A. Peres, Oxidation of *p*-hydroxybenzoic acid by UV radiation and by TiO$_2$/UV radiation: comparison and modeling of reaction kinetic, J. Hazard. Mater. B 83 (2001) 255–264.

[37] Y.M. Xu, C.H. Langford, Variation of Langmuir adsorption constant determined for TiO$_2$-photocatalyzed degradation of acetophenone under different light intensity, J. Photochem. Photobiol. A: Chem. 133 (2000) 67–71.

[38] Y.B. Meng, X. Huang, H.C. Shi, X.M. Wang, Y. Qian, N. Kubota, T. Endo, G. Fukunaga, Proceedings of the First Joint China/Japan Chemical Engineering Symposium, Beijing, China, September, 2000, pp. 201–202.

[39] J. Cunningham, G. Al-Sayyed, Factors influencing efficiencies of TiO$_2$ sensitized photodegradation substituted benzoic acids: discrepancies with dark-adsorption parameters, J. Chem. Soc., Faraday Trans. 86 (1990) 3935–3941.

[40] J.M. Kesselman, N.S. Lewis, M.R. Hoffmann, Photoelectrochemical degradation of 4-chlorocatechol at TiO$_2$ electrodes: comparison between sorption and photoreactivity, Environ. Sci. Technol. 31 (1997) 2299.

[41] C.G. Silva da, J.L. Faria, Photochemical and photo-catalytic degradation of an azo dye in aqueous solution by UV irradiation, J. Photochem. Photobiol. A: Chem. 155 (2003) 133–143.

[42] G. Rothenberger, J. Moser, M. Gratzel, N. Serpone, D.K. Sharma, Charge carrier trapping and recombination dynamics in small semiconductor particles, J. Am. Chem. Soc. 107 (1985) 8054–8059.